National Aeronautics and
Space Administration

HLS-PAP-025

REVISION A

RELEASE DATE: MAY 26, 2022

HUMAN LANDING SYSTEM (HLS) PROGRAM
WHITE PAPER
ACTIVE TERRAIN RELATIVE NAVIGATION FOR SUSTAINED LUNAR LANDING

REVISION AND HISTORY PAGE

Revision No.	Change No.	Description	Release Date
-		Initial Baseline Release	01/07/22
A		Replacing "LETS" with some version of "Artemis Sustained missions"	05/26/22

TABLE OF CONTENTS

SECTION **PAGE**

TABLE

FIGURE

1.0 MOTIVATION FOR ACTIVE TRN

Terrain Relative Navigation (TRN) is an autonomous spacecraft navigation function that provides absolute position estimates by matching sensor data collected on-board to a map generated from orbital reconnaissance. Two recent NASA missions have successfully employed visible camera based TRN (aka passive TRN) systems to accurately navigate to a desired target: OSIRIS-REx for asteroid surface sample acquisition [1] and Mars 2020 for large hazard avoidance during landing [2]. These techniques are passive in that they rely on the sun to illuminate the scene for successful landmark matching.

TRN techniques can be applied to lunar landing as well. After the de-orbit maneuver, the initial ground navigation-based position estimate degrades due to dead-reckoning during the long coast phase. This position error should be reduced by TRN to refine the spacecraft state just prior powered descent initiation. After the powered descent burn, TRN should be used again to clean up position errors that have accumulated. Due to the high altitude for these TRN updates, the onboard sensor data can be rather coarse leading to large errors in the position provided by TRN. As the lander descends, sensor data can be matched to maps of higher and higher resolution leading to accurate position estimates for landing. This sequence of TRN updates starts hundreds of kilometers down track from the landing site and for passive TRN, all this terrain must be illuminated.

The illumination along the descent trajectories to landing sites at the lunar South Pole is at best oblique and often non-existent. When the sun is present, the large terrain relief at the South Pole can cast long shadows which can inhibit landmark matching while an approach trajectory from the night side will be completely dark. Although it is possible to approach the South Pole during the day this would add an additional constraint on the already over constrained[1] set of HLS landing trajectories. Not surprisingly, studies show that around 50% of the landing trajectories would be eliminated if illumination is required along the descent trajectory. Given the landing cadence of the sustained missions and their delivered to the same region, this additional lighting constraint will be unacceptable.

Figure 1 shows a polar view of four NASA developed reference descent trajectories. The swath of a camera field of view looking nadir along each trajectory is shown in gray over a map of the fraction of the scene that is illuminated (Efficiency in the figure). The amount of illumination is directly correlated with the performance of passive TRN. If at least 40% of the scene is illuminated, then passive TRN should perform nominally but below that the performance in terms of accuracy and the ability to self-check the position estimates (robustness) degrades and then will ultimately fail. Three out of four of the trajectories (e.g., T1, T2 and T4) are in the dark for most of the descent and only encounter illuminated terrain when very close to the landing site. These trajectories are not viable, because performing TRN at the last moment will be challenging because large position errors will accumulate over time and correcting these errors will require very large and rapid maneuvers. The remaining trajectory (T3) is illuminated for much of the flight path, but there are still significant gaps when the lander flies over shadowed terrain.

[1] HLS landing trajectories are constrained by the arrival of HLS and Orion into the NHRO orbit as well as direct to earth telecom and landing site lighting for surface operations and power.

TRN approaches that use sensors that provide their own illumination can eliminate this lighting constraint. One approach that shows particular promise generates position fixes during descent by correlating lidar data collected on-board to digital elevation maps (DEMs) generated from orbital assets. In this Active TRN approach, the lidar provides its own illumination so TRN will work under any lighting conditions. This technique is not unprecedented, prior to GPS being widely available, cruise missiles used a system called TERrain COntour Matching (TERCOM) for accurate targeting [3]. More recently, the ALHAT program developed a proof of concept for lidar based contour matching and position estimation [4]. Although Active TRN is not as mature as passive TRN techniques, its benefit warrants near term development for HLS. The sections below describe a detailed state of the art point design for an Active TRN system and an approach to mature the technology to TRL 6 for flight implementation.

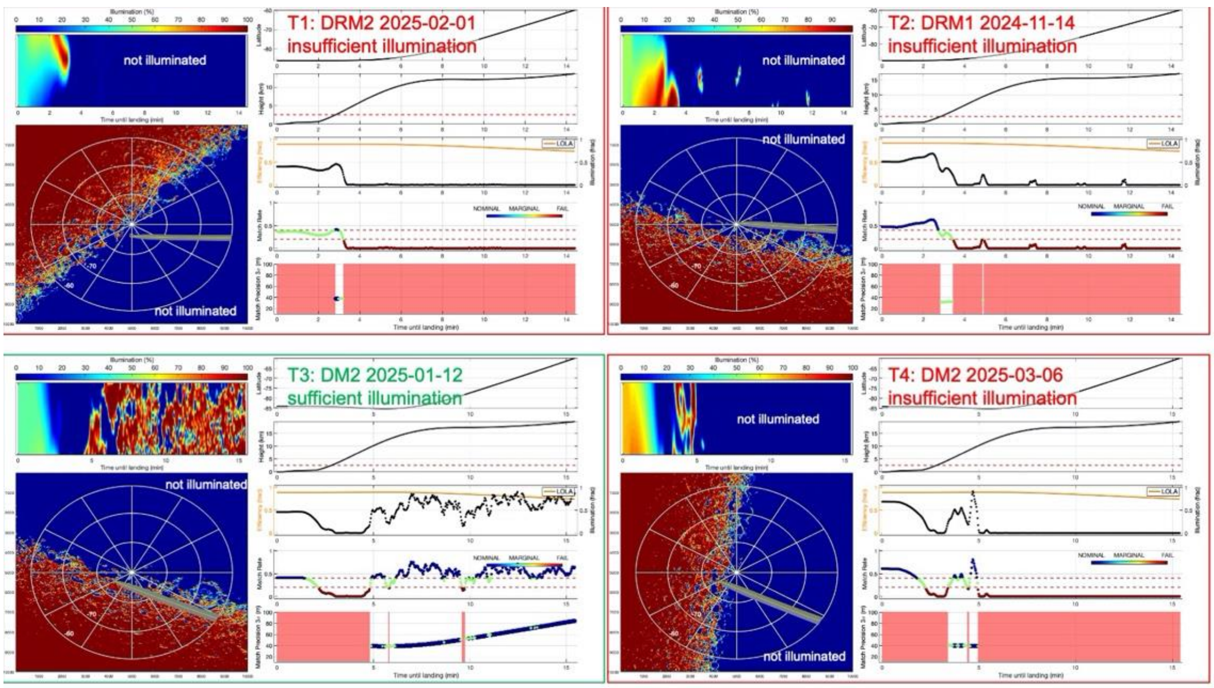

Figure 1: The illumination conditions for 4 example NASA descent trajectories.

2.0 ACTIVE TRN CONCEPT OF OPERATIONS

Active TRN takes advantage of the rapid horizontal motion of the lander to sweep a lidar across the lunar terrain (Figure 2). The lidar measures range at a constant rate and using the pointing knowledge of the lidar and the navigated spacecraft position, velocity and attitude estimates, these ranges can be turned into three dimensional points in a surface map coordinate frame. Regridding the points into an array of elevations turns them into an elevation contour that can be spatially correlated with an elevation map. The shift between the best matching location of the contour and its predicted location is a measurement of the position error between the spacecraft and the map.

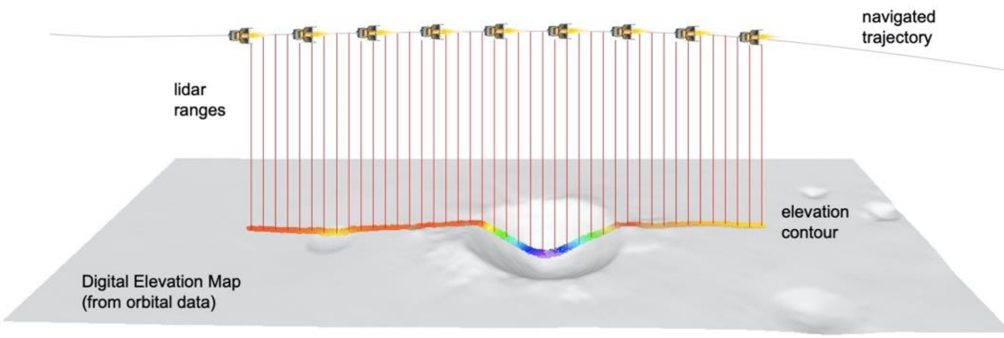

Figure 2: Active TRN concept.

A block diagram composed of sensors, avionics, and software for a flight implementation of Active TRN is shown in Figure 3. Given the update rates required, Active TRN will require more processing than is available from a standard flight computer (e.g., BAE RAD750). One option, as shown in Figure 3, is to develop a stand-alone compute element for TRN. This allows the TRN function to be tested separately from the rest of the spacecraft avionics but is not strictly necessary if additional co-processing resources are available within the spacecraft compute element.

The TRN computing interfaces to the lidar for range data, the IMU for angular rates and accelerations, and spacecraft compute element for the initial spacecraft navigation state. During Active TRN, the initial spacecraft state is propagated forward with IMU data by the TRN navigation software. This internal navigation state is provided to the Active TRN software which generates a contour from the lidar ranges, matches it to the elevation map and provides a position estimate back to the navigation software. The navigation software provides a position correction back to the spacecraft compute element. This position correction can be applied to the spacecraft navigation state or the location of the landing target as was done for Mars 2020 TRN [5]. Although two navigation filters are running in this architecture, they are only loosely coupled through the shared IMU data. A single spacecraft state initializes the TRN navigation software which then operates independently to generate the position correction. This approach enables testing of TRN independently from the spacecraft avionics.

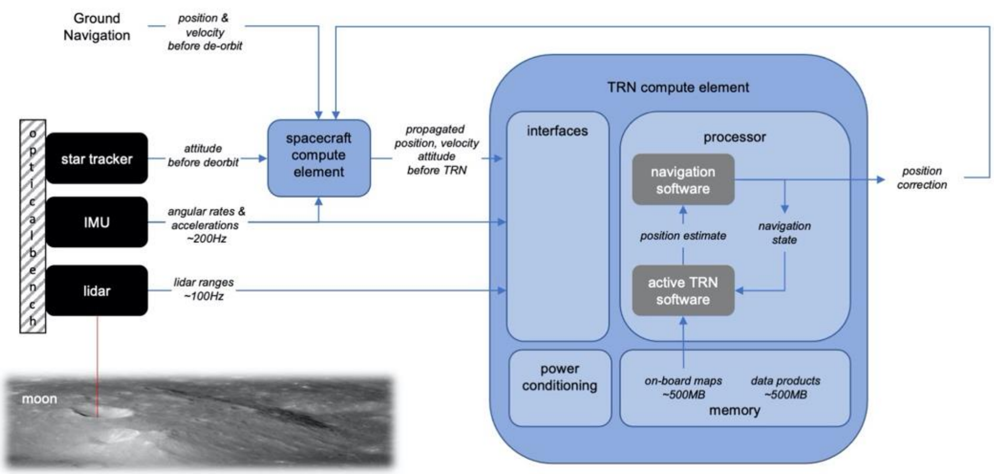

Figure 3: Active TRN flight block diagram.

Active TRN fits into Deorbit, Descent and Landing (DDL) as follows. Prior to descent, the lander is in orbit around the Moon and can obtain ground-based navigation updates of position and velocity. Inside the spacecraft compute element, these are combined with star tracker-based attitude measurements to provide a complete spacecraft navigation state estimate (position, velocity and attitude) prior to de-orbit. A burn is used to de-orbit the lander and during this maneuver and coast to the surface Inertial Measurement Unit (IMU) data is propagated to maintain navigation state. Position errors accumulate during the coast phase, so Active TRN should be applied to remove position errors and enable more accurate targeting prior to Powered Descent Initiation (PDI) which occurs, as shown in Figure 4, around 400km downrange. Ideally, Active TRN is performed continuously from that point forward, but at the very least should be applied periodically to prevent position error growth and to reduce the position errors using higher resolution reference DEMs.

Reference DEM pixel size is the primary driver on position error for Active TRN; smaller pixel sizes result in lower position errors. DEMs of the South Pole derived from the Lunar Reconnaissance Orbiter (LRO) Lunar Orbiter Laser Altimeter (LOLA) range measurements are publicly available [6]. Because these maps are seamless, global and have been extensively verified, they are an excellent starting point for the Active TRN reference DEM. Due to the polar orbit of LOLA, the density of lidar points increases toward the pole, and, consequently, the pixel size of derived DEMs decreases. Figure 4 shows an elevation map of the South Pole with the LOLA DEM pixels size in meters per pixel (mpp) as a function of latitude. The RA17 and Malapert trajectories always move toward the pole during descent, so the LOLA DEM pixel size will decrease and the Active TRN position error will also decrease. However, the trajectories to DM2 approach the pole and then move away so the Active TRN position error will decrease but then increase near the landing site. This increase can be mitigated by bringing in higher resolution DEM data sources along the trajectory (e.g., Kaguya Terrain Camera [7] or LRO Narrow Angle Camera stereo pairs [8]) if they are available.

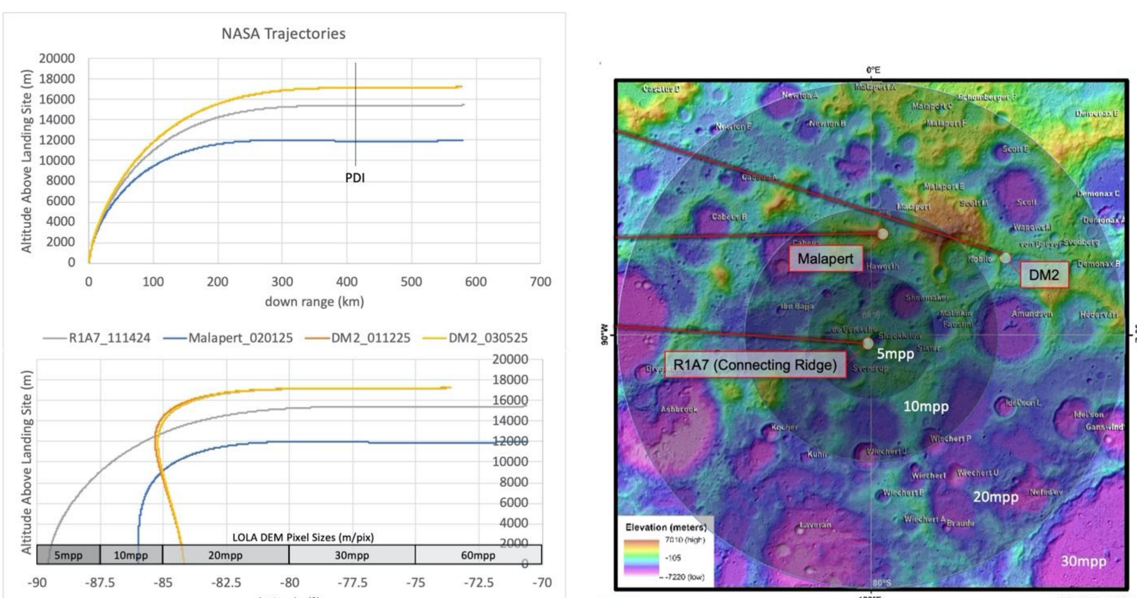

Figure 4: Example NASA trajectories during Active TRN operation and LOLA DEM resolutions versus latitude.

3.0 LIDAR REQUIREMENTS AND DESIGN

An imaging lidar is not required for Active TRN; a laser altimeter will suffice albeit one with long range and moderate pulse rate. The maximum range of the lidar is set based on the altitude and pitch during Active TRN operation and the lunar terrain relief. For the NASA reference trajectories, the altitude of the lander prior to PDI can be between 15km and 20km above the lunar ellipsoid. During descent the lander pitches approximately 30˚ which can increase the required range. These effects combined with +/- 7km of terrain relief at the lunar South Pole indicate that the lidar should have a maximum range of 30km. The maximum range should account for the lunar reflectivity and the steep slopes present at the South Pole.

The lidar pulse repetition frequency (PRF) or points per second should be high enough that there is at least one lidar measurement in each DEM pixel so that the contour is without gaps and terrain features are not missed. Using the four NASA reference trajectories and the LOLA DEMs, a PRF of 100Hz is sufficient. For the R1A7 there is a time when a 100 Hz PRF is not quite high enough given the high horizontal velocity when entering the 5mpp LOLA map, but this can be compensated by using the 10mpp DEM for a while longer; there will still be plenty of time over the 5mpp map for it to be used for Active TRN.

The divergence of the lidar should be set so that the beam is no wider than one DEM pixel. If the beam is greater than a pixel then the contour will be a smoothed or noisy version of the DEM elevations which in either case could impact correlation of the contour. Because the terrain is continuous, a beam that is smaller than a pixel will still represent an elevation within a single pixel and should not affect correlation; testing with real data is needed to prove this. Once again using the NASA trajectories and the LOLA DEMs, a divergence of 0.5mrad full width is sufficiently small to keep the beam smaller than 1 pixel for the highest resolution DEM available along the trajectory.

The lidar range noise needs to be sufficiently low to enable accurate and robust correlation given the terrain relief expected. A sensitivity study with increasing range noise was performed using an Active TRN simulation described later. The simulation results over 5mpp LOLA DEMs showed that matching performance begins to degrade when range noise is 1m 3-σ. Backing off from this the simulation showed no performance degradation for 0.5m 3-σ range noise.

A summary of these key requirements on the lidar are given in Table 4-1Table 4-1. A survey of commercial products did not turn up any lidars that meet these requirements however, there are a few lidars in development by space agencies that come close. For example, the NASA LOLA instrument can achieve the range and its 28Hz rate combined with the 5 spots per laser pulse would allow that design to meet requirements with some modifications. The MacDonald, Dettwiler and Associates OSIRIS-RE-x Laser Altimeter instrument that flew on OSIRIS-REx fired at 100Hz and had a maximum range of 9km, but that was to the very dark Bennu asteroid (albedo of 0.046). A maximum range of 30km to the brighter lunar surface (albedo between 0.2 and 0.4), should be achievable. There are other examples as well but these two clearly show that building a lidar to meet the requirements will not require technology breakthroughs and instead is a methodical engineering development.

TABLE 4-1: ACTIVE TRN LIDAR DRIVING KEY REQUIREMENTS.

Parameter	Value	Rationale
Maximum range	30km	Enables ranging prior to powered descent initiation to the lowest terrain at the lunar South Pole.
Points per second	100Hz	Enables placement of a single point in each DEM pixel used for correlation and position estimation
Beam Divergence	< 0.5mrad full width	Keeps the lidar spots from being greater than 1 DEM pixel
Range Noise	< 0.5m 3σ	Necessary to enable accurate contour matching for 5 meter per pixel DEMs

4.0 ON-BOARD DATA PROCESSING

The fundamental measurement made by Active TRN is the position shift between a sequence of lidar ranges and a digital elevation map. The Active TRN algorithm that produces these measurements should be accurate, computationally efficient, and not produce incorrect answers in the presence of lidar noise, navigation state and map errors, and bland terrain. An example algorithm developed by NASA JPL is shown in Figure 5 and described next.

The Active TRN (aka Lidar TRN) algorithm takes as input timed lidar ranges, a reference DEM and a predicted spacecraft trajectory from a navigation filter, and it outputs a spacecraft position measurement in the reference DEM frame.

In lidar contour construction, the lidar ranges are first converted to 3D points using the pointing vector of the lidar in the spacecraft frame. A spacecraft pose is interpolated for each lidar measurement and used to transform the lidar points into the reference DEM coordinate frame. An empty map of elevations is then allocated and the elevation of each lidar point is inserted at the corresponding pixel in the map. If multiple points fall in a single pixel, then their elevations are averaged.

The lidar contour is not guaranteed to follow a straight line of pixels due to spacecraft attitude motion and terrain relief, but a sequence of connected pixels can be extracted and put in linear array. An edge detector is applied to this array to improve correlation by emphasizing changes in elevation.

The reference DEM is cropped based on the current position estimate and bounds on position error. For each proposed match location in the DEM (a rectangle of DEM pixels), an array of elevations is extracted that follows the sequence of pixels in the lidar contour albeit centered on the proposed match location. This map elevation contour is run through the edge detector and the correlation coefficient with the edge filtered lidar contour is computed. Looping through the possible match locations creates a correlation surface. A sub-pixel fit is applied to the highest correlation peak to generate the best match location. Correct matches should have peaks that satisfy thresholds on peak height, peak width, and the ratio of the highest to second highest peak. However, studies have shown that these correlation metrics are weak indicators of correct matches; setting them tight enough to throw out all false matches will also throw out many correct matches.

Geometric consistency-based outlier rejection circumvents this problem. The contour is broken into multiple disjoint sub-contours, and each is correlated with the reference map to generate multiple match pixel locations. Assuming the position error does not change significantly between each sub-contour, which is a valid assumption for lunar landing and the short times required for contour generation, all the position corrections will be similar. A threshold is set using the estimated navigation state covariances and expected correlation accuracy to separate correct from incorrect matches. All match measurements that are within the threshold of one of the matches form a consistent set. If the largest consistent set contains at least half of the sub-contours then the measurement is considered valid and can be used for navigation.

The position corrections from the multiple sub-contours are averaged and provided back to the navigation filter which ingests it as a measurement. The navigation filter can be a sequential filter with rather simple update equations given the 3D nature of the measurement. Moving batch filters that combine a sequence of position updates can also be used. Couplings between the Active TRN algorithm and the navigation filter should be studied and appropriate fault protection to prevent filter divergence should be implemented.

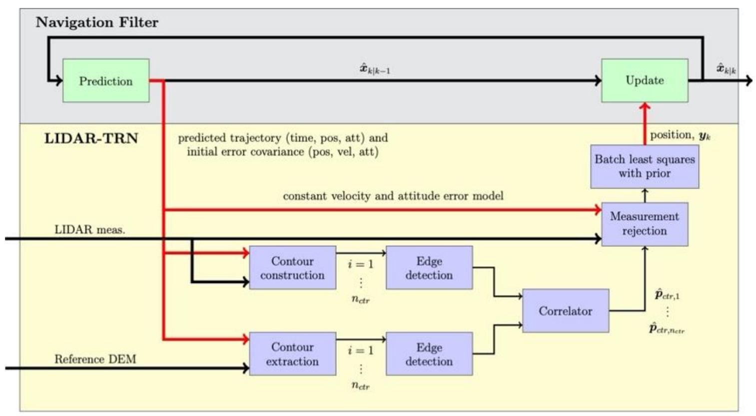

Figure 5: Active TRN algorithm block diagram.

Figure 6 shows an example of Active TRN where geometric consistency detected an incorrect sub-contour match. The edge filtered sub-contours are shown in the lower left and correlation surfaces and metrics on the right. All three sub-contours have acceptably high correlation peaks and narrow widths. The peak ratio for one of the cases is lower than the other two but still above threshold. However, when applying the geometric consistency check, this match does not agree with the others and is thrown out. A valid measurement is still made because a majority (2 out of 3) of the matches agree. The upper left diagram shows the match locations for all three sub-contours.

The Active TRN algorithm requires 3D geometric floating-point calculations and correlation of a nonlinear contour across a large area. To assess processor requirements, the algorithm was coded in C and then ported to a Xilinx Zynq Ultrascale DS891 development board. The run-times, using a 20mpp reference DEM, on a single ARM A53 processor core for different position errors (x-axis) and contour lengths (different curves) are shown in Figure 7. The run times range from 11s to a small fraction of a second.

Simulations have shown that a 9km contour with 3 sub-contours is long enough to guarantee valid answers for 20mpp south polar lunar terrain. A typical initial position error (the error to be removed by Active TRN) for 20mpp maps is less than 1500m. For these algorithm parameters, Active TRN processing takes 1.3s to process; each sub-contour takes 0.4s and the outlier rejection and position estimation takes 0.1s. If larger position errors are present, then the run-times will grow quadratically, but once Active TRN is run, the errors will decrease along with a reduction in run-time. If longer contours are needed, then the run-time will grow linearly.

The nominal 1.3 s run-time is a fraction of the data collection time (~6s) so it is not limiting the Active TRN update rate. However, this benchmark shows that processing on order that which is provided by a single ARM A53 core on a Zynq Ultrascale is required for Active TRN, a typical flight processor (e.g., BAE RAD750) will not be sufficient.

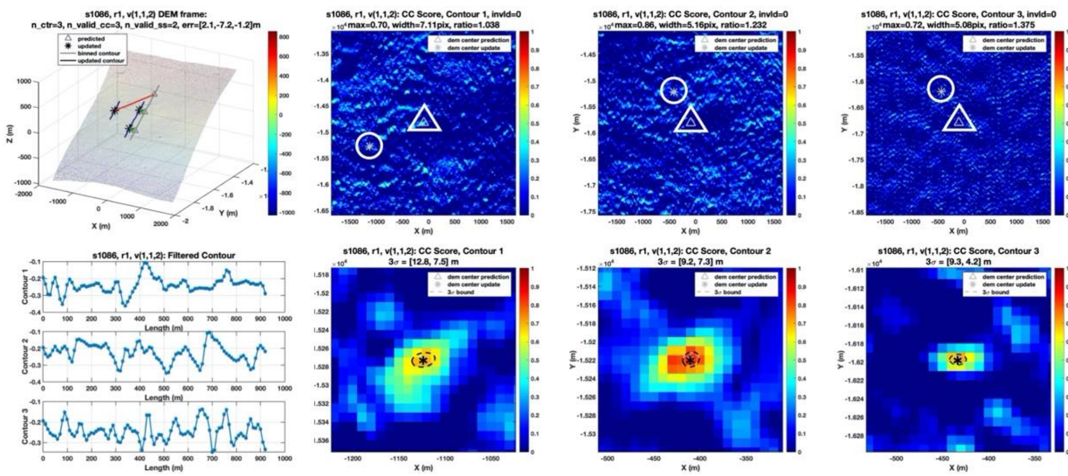

Figure 6: Active TRN algorithm example with simulated data.

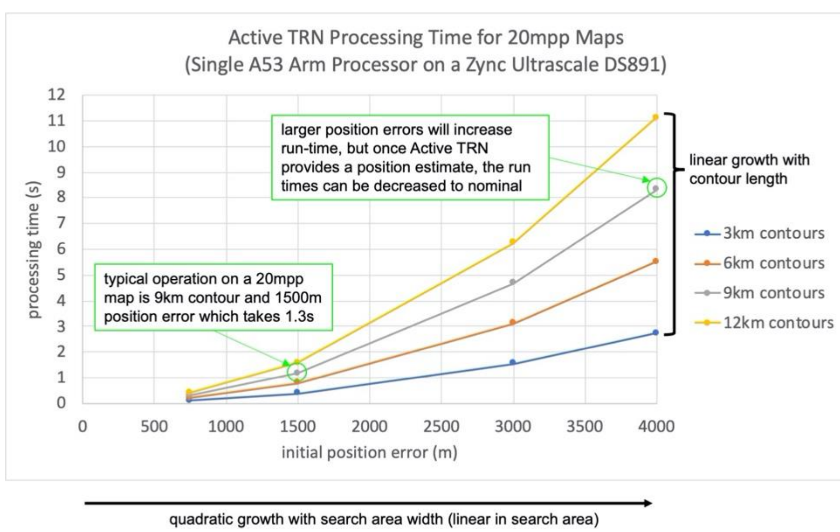

Figure 7: Active TRN processing time on an ARM A53 processor.

5.0 EXPECTED PERFORMANCE

A high-fidelity simulation shown in Figure 8 was developed to assess Active TRN performance. The algorithm takes lidar points, navigation state and an onboard map each with their own set of errors. The lidar model generates ranges to a surface using ray tracing. The divergence of the lidar beam is modeled by measuring range to the truth map for multiple rays emanating from the sensor across the beam. The range detection electronics of the lidar can be modeled by processing the ranges in different ways; currently average range and first return are modeled. Gaussian noise and a bias can be added to the ranges. The lidar follows the truth trajectory and collects ranges at the specified sample rate. The truth trajectory is also provided to the trajectory model with adds biases and gaussian noises to generate the navigated position, velocity and attitude. The true map is currently a subset of a LOLA DEM at a specific map pixel size and centered on a specific latitude and longitude. The true map is distorted locally which moves features in the map relative to each other.

The nominal values used in the simulation are shown in parenthesis in Figure 8. Sensitivity studies have shown that the driving simulation parameters on position estimation performance are attitude errors and local map distortion. Attitude error was set to 0.1˚ 3σ which should be achievable with a star tracker and high quality IMU expected for the landers. A map distortion of 1 map pixel for short ranges and 2 map pixels for long ranges is consistent with the distortion seen in Mars 2020 TRN maps and is expected to also be achievable for lunar maps.

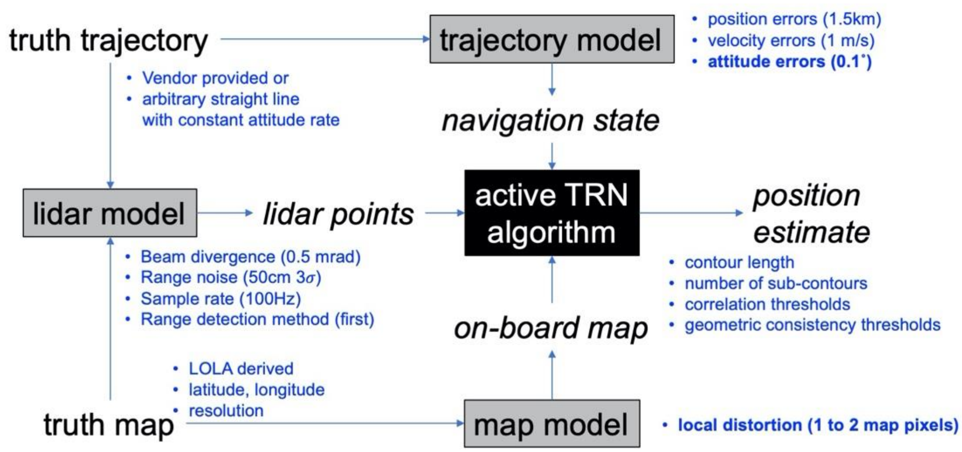

Figure 8: Active TRN simulation block diagram with parameters that can be modified.

The simulation was used to assess position estimation accuracy and robustness for lunar terrain at different latitudes and LOLA reference map pixel sizes. First a sensitivity study was performed to determine the shortest contour that always provided a valid position error. For 20mpp maps this turned out to be a 9km contour (i.e., 450 pixels) broken into 3 sub contours. This 450-pixel contour rule of thumb was used to set the contour lengths for the other map pixel sizes. 2000 cases were generated for maps of different map pixel sizes and corresponding contour lengths: each map pixel size had LOLA derived maps from 8 different longitudes, within each map 25 different locations were investigated, and each of these had 10 different random seeds for setting lidar, map and navigation trajectory noises.

Table 6-1 shows the position estimation results. In all 10,000 cases there were no invalid results; active TRN always gave an answer, and the answer was correct. Position errors on order 1 map pixel are typical however judicious margin should be assumed at this point in development. Margined position errors are shown on the right in the table which are less than 3 map pixels in all cases. As described in the Con-Ops above, Active TRN is applied to maps of decreasing map pixel size as the spacecraft approaches the landing site. As shown in Figure 9, the R1A7 (Connecting Ridge) trajectory can use 5mpp maps and achieve a position error of 20m. The Malapert landing site is farther from the pole, so the best resolution LOLA DEM is 10mpp resulting in a 30m Active TRN error. Finally, for the DM2 landing sites, the spacecraft descends over the 10mpp DEM latitudes and can achieve a 30m Active TRN error. However, the spacecraft then moves away from the pole and into the 20mpp LOLA DEM which will result in a greater Active TRN position error. For all the trajectories, the Active TRN error is sufficient to achieve the 50m sustained mission landing accuracy requirement assuming error propagation from the last TRN error is not too large. As mentioned in the Con-Ops section, if more accurate Active TRN errors are needed then potentially LROC NAC derived DEMs near the landing site can be constructed and validated for use as Active TRN reference maps.

TABLE 6-1: ACTIVE TRN POSITION ESTIMATION PERFORMANCE WITH RESPECT TO MAPS AND ALTITUDE.

Map and Trajectory Parameters			Contour Parameters			**Horizontal Position Error**			
map latitude range (˚S)	map pixel size (m)	Altitude (km)	sub contour length (km)	# sub contours	total contour length (km)	**# invalid cases**	**sim 99%tile (m)**	**sim max (m)**	**99%tile margined (max*1.5) (m)**
60-75	60	15	9	3	27	**0**	**50.0**	**69.8**	**105**
75-80	30	15	4.5	3	13.5	**0**	**32.3**	**47.1**	**70**
80-85	20	15	3	3	9	**0**	**28.5**	**32.7**	**50**
85-87.5	10	7.5	1.5	3	4.5	**0**	**15.6**	**19.0**	**30**
87.5-90	5	3.75	1	3	2.25	**0**	**8.7**	**12.4**	**20**

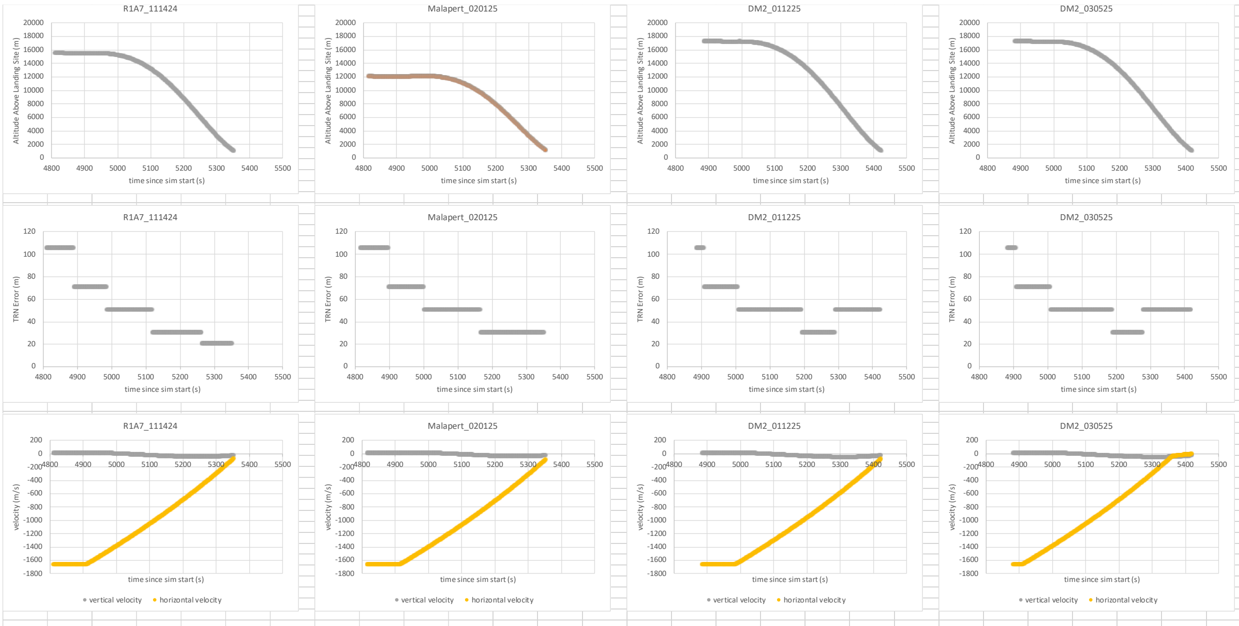

Figure 9: TRN accuracy (middle plots) for 4 NASA trajectories given simulation performance results in Error! Reference source not found.**.**

6.0 TECHNOLOGY MATURATION APPROACH

Active TRN has been tested with real data [4] and in a high-fidelity lunar simulation. The algorithm has also been shown to run in adequate time on a potential flight processor. These advances place Active TRN at Technology Readiness Level 4 (Component and/or breadboard validation in laboratory environment). Although Active TRN appears feasible there is still development risk. This risk could be retired quickly prior to Sustaining Lunar Development PDR with a robust technology development task that matures Active TRN from TRL 4 to TRL 6 (System/subsystem model or prototype demonstration in a relevant environment).

Using the Mars 2020 Lander Vision System (LVS) technology development as a model, there are four steps to this maturation.

Active TRN is more than just a lidar or an algorithm; it is the algorithm, lidar, IMU, avionics and software all working in real-time to estimate position. So, the first step is to develop and finalize the design of the Active TRN system and create a simulation to match the design.

Integrate and test a real-time prototype Active TRN System that matches the design but uses existing or COTS components that have path to flight implementation. If necessary environmental testing should be used to prove a component is ready for flight implementation.

Perform a terrestrial field test of the real-time prototype Active TRN System to demonstrate position accuracy can be met and to also validate the simulation across a wide range of altitudes and terrains.

Use the validated simulation to assess Active TRN performance across the entire lunar descent operational envelope.

Figure 10 shows an example prototype Active TRN system. It closely follows the flight design albeit with some COTS components when appropriate to reduce development cost. All of the sensors are mounted on a rigid optical bench so precise alignments can be maintained. An INS/GPS is the ground truth trajectory sensor and, after appropriate errors are added, it can also replace inputs from ground navigation and the star tracker. Given the short propagation times, a COTS tactical grade IMU (e.g., a Northrop Grumman LN-200) should suffice. A COTS truth lidar, with potentially lower sample rate, should be co-boresighted with the Active TRN lidar so it can be used cross check the ranges.

The sensors feed the prototype avionics which should contain a processor with a path to flight implementation and memory for maps and data products. Because of the feedback loop between the navigation filter and the active TRN contour matching, both algorithms should be run in real-time on the processor. The reference maps can come from terrestrial sources, but may need to have distortions and errors added to replicate the quality of the lunar maps.

Figure 10 also defines the risks that will be retired with this approach. First, a lidar design that meets the Active TRN requirements exists and can be space qualified. Second, Active TRN contour matching and navigation filter algorithms exist that meet accuracy and robustness requirements, and the coupling between them does not have any untoward consequences like navigation state divergence over time. Third, active TRN has an update rate that meets requirements on a processor that is comparable to one that will be used for the flight system. Fourth and finally, it will demonstrate that an accurate and robust end-to-end real-time active TRN function can be implemented for HLS.

The specific hardware used for the Active TRN prototype will depend on implementation constraints specific to the HLS vendor. As stated before, building a lidar that meets the Active TRN requirements is an engineering development with low risk that multiple companies and organizations could implement. Furthermore, there are multiple paths to providing the necessary processing power for Active TRN, but whatever approach is used should take advantage of the other avionics development at the HLS vendor.

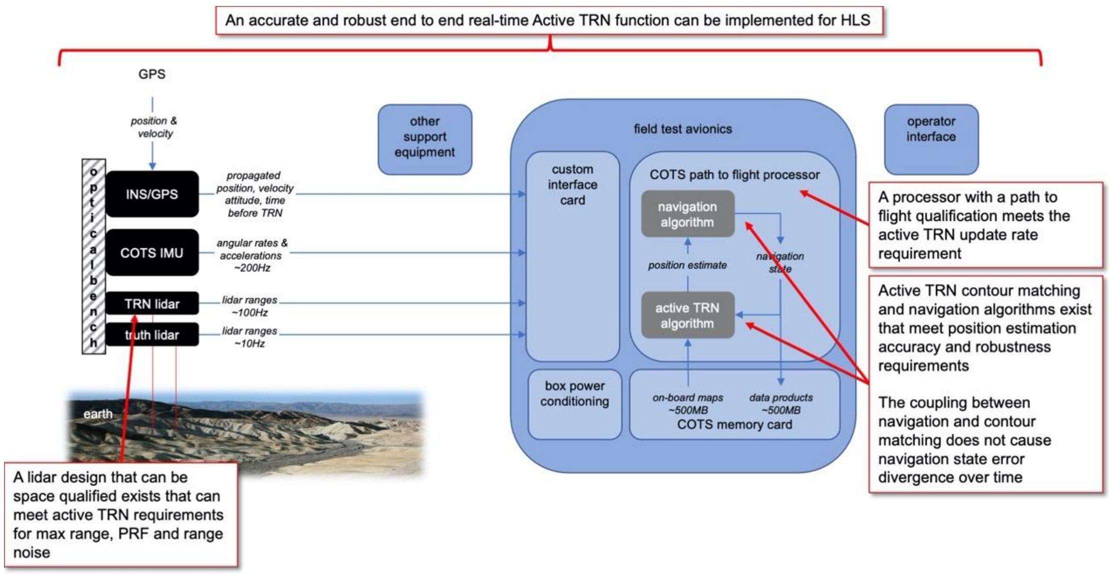

Figure 10: Active TRN Prototype block diagram.

Although there is some flexibility on the choice of lidar and processor, there is a clear platform of choice for field testing. The field test vehicle should cover as much of the Active TRN operational envelope as possible so that direct comparisons can be made to simulation results and flight conditions. Table 7- compares multiple vehicles used for past field tests of Entry Descent and Landing (EDL) technologies against some key Active TRN parameters shown on the left. The helicopter platforms only cover part of the altitude space and none of the horizontal velocity space. The Controlled Descent System used for the Mars Phoenix radar testing does achieve the necessary vertical velocities, but that platform has not been used in more than a decade and would need significant rework to become operational. Vertical Take-off Vertical Landing (VTVL) vehicles typically go up and then come down close to the launch pad. It is conceivable that these vehicles could be operated with larger horizontal motion, but each flight would only cover a limited swath of terrain at a very high cost for each flight. The fixed wing aircraft are the better options given the altitudes, velocities, and terrain coverage possible.

A fighter jet is the best option because it can fly at significantly higher horizontal velocities and altitudes when compared to a turboprop. Figure 11 shows the coverage of the Active TRN velocity and altitude space by an F18 fighter jet available from NASA Armstrong Flight Research Center [9]. The F18 can fly near to the ground at high horizontal velocity which allows it to match the conditions of Active TRN for the highest resolution maps near the landing site. Because these are the final TRN measurements before landing, they are the most critical for achieving low touchdown error and achieving “test as you fly” for these conditions will be a very convincing risk reduction. The F18 cannot achieve the 1700 m/s present during lunar landing, but for that part of the test space, lidar ranges can be skipped so that the ground spacing of lidar points along the contour is the same as it would be for lunar landing. This might even be more stressing since the IMU will be propagated for a longer time and more errors in the navigated trajectory will accumulate.

Field testing matures Active TRN in multiple ways. The comparison of range measurements to the truth lidar data and digital elevation maps verifies the lidar meets requirements. The Active TRN simulation can be configured with field test truth maps and trajectories and the results compared to actual field test runs. Finally, for a top-level validation of the simulation, the scatter plot of position errors from all the field test runs at a specific map pixel size can be compared to lunar simulation runs at the same map pixel size. Once the simulation is validated it can be used to cover the entire operational envelope of Active TRN to quantify performance for lunar landing.

7.0 SUMMARY

Sustained missions require landing under any illumination conditions which precludes the use of passive TRN. Active TRN is a viable alternative that can meet the 50m landing accuracy requirement and do so under any lighting conditions. An Active TRN algorithm and software implementation has been tested but more work is needed to retire developmental risk and bring an Active TRN which includes a lidar, algorithms, IMU, avionics and software to system to TRL 6 prior to a Sustaining Lunar Development PDR.

TABLE 7-1: FIELD TEST PLATFORM COMPARISON.

Metric \ Venue	Helicopter, Captive Carry (A-Star AS350B3E)	Helicopter, Controlled Descent System (Bell 205A)	Fixed Wing Turboprop (Beech B200C)	Fixed Wing Jet (F-18)	VTVL (Masten Xogdor) Avaiable NET 2023	VTVL (Blue Origin New Shepard) Availability TBD
Max Altitude (m, MSL) requirement: 18000	**5000**	5900	10700	15000	120000	100000
Max Horizontal Speed (m/s) requirement: 1700 m/s to 80 m/s	70	61	133	375	200	TBD
Max Vertical Speed (m/s) requirement: 0 to 60 m/s	1.5	61	20 m/s	700	200	1000
Portion of flight envelope that matches actual descent trajectory	no	no	no	yes	maybe if long traverse	not likely given vertical profile
Platform Ready	yes	would need to be resurrected	yes	yes	no	yes
Cover Variety of Terrain Types and Altitudes	yes	yes, but limited drops	yes	yes	very limited unless a long traverse is possible	no, west Texas terrain
Cost	low	low	moderate	moderate	high	high

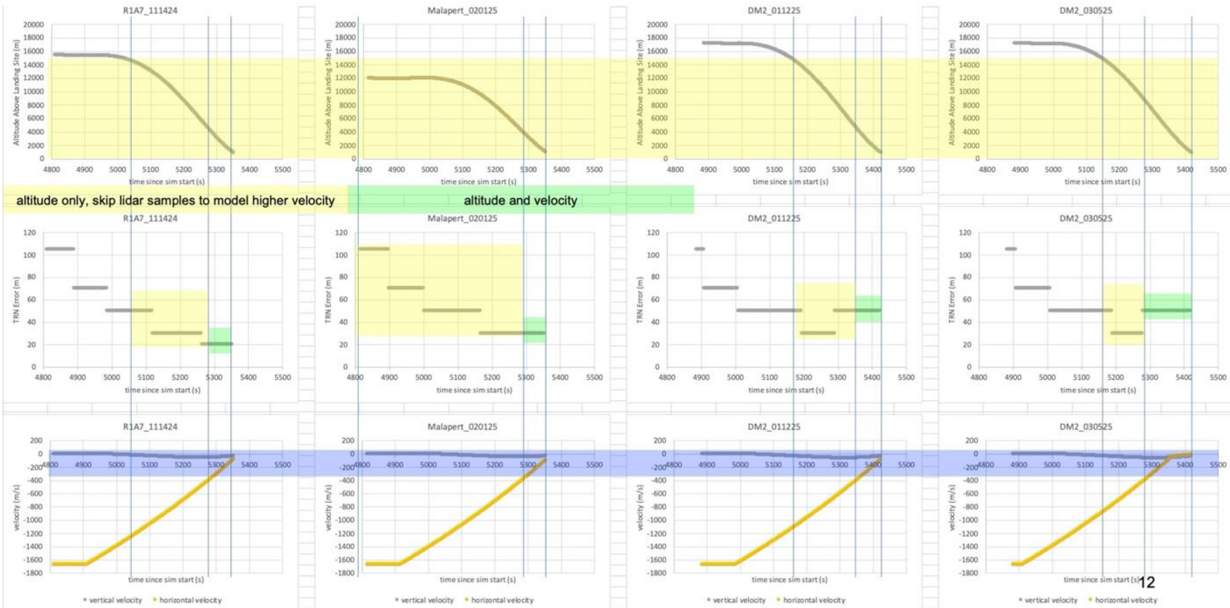

Figure 11: F18 coverage of NASA trajectories.

8.0 REFERENCES

[1] Miller, C. Olds, R., Norman, C., Gonzales, S., Mario, C., and Lauretta, D., "On-Orbit Evaluation of Natural Feature Tracking for OSIRIS-REx Sample Collection," *Proc. AAS Guidance Navigation and Control Conference*, AAS-20-105, AAS, Breckenridge, CO, February 2020.

[2] Johnson A. et al., "Mars 2020 Lander Vision System Flight Performance," AIAA SciTech Forum 2022, January 2022 (To Appear).

[3] Golden, J. P., "Terrain Contour Matching (TERCOM): a Cruise Missile Guidance Aid," *Image Processing for Missile Guidance, Proc. of the Society of Photo-optical Instrumentation Engineers,* Vol. 238, 1980, pp. 10-18.

[4] Johnson, A., and Ivanov, T., "Analysis and Testing of a LIDAR-Based Approach to Terrain Relative Navigation for Precise Lunar Landing," *Proc. AIAA Guidance Navigation and Control Conference*, AIAA, San Diego, CA, August 2011.

[5] Brugarolas, P. "Guidance Navigation and Control for the Entry Descent and Landing of the Mars 2020 Mission", *AAS Guidance Navigation and Control Conference* (AAS-17-031), AAS, Breckenridge, CO, 2017.

[6] "Moon LRO LOLA DEM 118m v1," URL: https://astrogeology.usgs.gov/search/details/Moon/LRO/LOLA/Lunar_LRO_LOLA_Global_LDEM_118m_Mar2014/cub [retrieved 7 December 2021]

[7] Haruyama, J. & Ohtake, M. & Matsunaga, Tsuneo & Morota, Tomokatsu & Honda, Cion & Yokota, Yasuhiro & Ogawa, Y. & Group, Lism. "SELENE (Kaguya) Terrain Camera Observation Results of Nominal Mission Period," *40th Lunar and Planetary Science Conference*, Abstract 1553, 2009.

[8] Robinson, M.S., Brylow, S.M., Tschimmel, M. *et al.* Lunar Reconnaissance Orbiter Camera (LROC) Instrument Overview. *Space Sci Rev* **150,** 81–124 (2010).

[9] Montgomery, J., "Implementing the Mars Science Laboratory Terminal Descent Sensor Field Test Campaign," February 2012, URL:

https://trs.jpl.nasa.gov/bitstream/handle/2014/42798/12-0593_A1b.pdf?sequence=1&isAllowed=y [retrieved 7 December 2021]